NINTH EUROPEAN ROTORCRAFT FORUM

Paper No. 20

AERODYNAMICS OF DUCTED COMPOSITE COUNTERROTATING ROTORS

Dino Dini

Istituto di Macchine
Università di Pisa

ITALY

September 13 - 15, 1983

STRESA, ITALY

Associazione Industrie Aerospaziali

Associazione Italiana di Aeronautica e Astronautica

AERODYNAMICS OF DUCTED COMPOSITE COUNTERROTATING ROTORS

by

Dino Dini

Istituto di Macchine
Universitã di Pisa (Italy)

ABSTRACT

As we look ahead at the many possibilities for new kinds of helicopter rotors, various altervatives for drive systems and vehicles having combinations of lifting rotors and thrust jet engines are analyzed.
To achieve a promising concept, a complete integration between engine and rotor design is proposed, in which a composite ducted lifting rotor is using counterrotating blade rings, over fixed geometry stator vanes to give always axial exit flow velocity in hover and forward flight.
This composite ducted rotor configuration, with jet engines for forward flight, permits considerable flexibility and yields high speed flight as well as high hover efficiency.
The ducted rotor/stator eliminates the reverse flow on the inner portion of the retreating blade rings.
Referring to hover, axial and forward flight, physical description of effects of the through-flow is investigated, before dealing with the dynamic-stability problem.
A method is given for calculating the behaviour in forward flight on the assumption of a composite rotor regarded as lifting surface. Performances are examined.
Problems are discussed, arriving at relatively sinple formulae which are not only useful in preliminary design, but which also enable a physical interpretation of the dynamic and aerodynamic phenomena.
It is proposed the development of an integrated lift/propulsion system, driving the ducted rotors and the propulsors through a combined transmission. Improvements are required in rotor blade and vehicle aerodynamics.

AERODYNAMICS OF DUCTED COMPOSITE COUNTERROTATING ROTORS

by

Dino Dini

Istituto di Macchine
Università di Pisa (Italy)

1. TOWARD NEW KINDS OF HELICOPTER ROTORS

Present new technology helicopters are already penetrating the fixed wing executive market, because of their largely improved economy, reliability, all weather capability and passenger comfort. During the past decade, remarkable progress has been made in the development of new rotorcraft to meet an increasingly diverse demand for vertical take off and landing capability. Significant for the future is the progress that has been made in the research and technical development for advanced rotorcraft and powered lift aircraft that will have substantially better performance than present generation of vertical flight aircraft.

The next decade will see technological developments of the compound helicopter and the lift-fan and augmentor thrust approaches to vertical flight, for an increasing use of rotorcraft and powered-lift VTOL.aircraft in a wide spectrum of civil and military applications. The cruise speed and efficiency of the compound helicpters (i.e., vehicles with some combination of rotor,wing, and auxiliary propulsion) will be increased primarily through various approaches that avoid the limitations of the retreating blade stall that characterizes the simple helicopter.

Where a combination of lifting and transportation is necessry, in which hover and cruise performance are important, the compound helicopter, using a combination of rotors wings or auxiliary propulsion, appears to have substantial promise.

Many new unique rotor configuration are being considered, and among them:

1) the articulated rotor hub is complex and composed of many parts. To reduce complexity and weight, elastomeric materials are being introduced for use as the hinge components. Another approach eliminates the hinges entirely with a rigid hub. In addition to eliminating a large number of moving parts, the hingeless rotor has great potential for improvement of flying qualities. Application of new materials, particularly composite, will enable the relative stiffnesses of the rotor (chordwise, beamwise, and spanwise) to be tailored to provide

optimum structural dynamic characteristics. New materials, as well as improved fabrication techniques, will also permit a much wider latitude in optimization of blade external geometry to improve performance. These concepts are not without concomitant difficulties, because bearings rotors introduce structural coupling that tend to make the vibrational loads and aeroelastic stability problems more severe. A primary influence on the performance of rotorcraft is the installed power train from engine through transmission. An increase in loads capacity will evolve from advanced gear tooth forms, new gear materials, improved tooth surface finish, improved profile tolerance, new lubricants with increased load capacity and improved methods of manufacturing. Design and development of drive systems have become systematized and analyzed more rigorously be new analytical approaches, for entering fleet service with an increased assurance of meeting cost, safety, and noise goals to the direct benefit of the user. Numerous studies have given clear indications of the mechanism responsible for the generation of noise within a gearbox, in the frequency domain between 300 and 5,000 hertz. Resonances of the gearbox casing and/or the gearbox components can be avoided or shifted in frequency, by relocating the position of bearings, changing the bearing stiffness or changing the shaft stiffness or mass distribution. Vibration reduction is obtained through changing the tilt of the rotorcraft in forward flight to achieve minimum cyclic induced flapping of the rotor blades. Vibration absorbers, nodal systems and vibration isolators will have to be utilized to decrease vibrations further, in particular when high vibration levels are incurred with hingeless rotor systems, which cannot be completely removed by tilting the rotorshaft in flight. The use of composite materials in combination with elastomers is gaining attention, with increased noise;

2) the cumulative effect of innovative technology is to meet the challenge of the 1980's, when vertical flight is taken for granted, and success or failure is measured by return on investment. Among the principal factors pulling technology are new rotary wing configurations, with reflection in technological objectives over a spectrum of disciplines involving improvements in aerodynamic efficiency and aeromechanical stability, reductions in vibration and noise, increased agility and precision of flight control, attainment of a level of safety, improved structural efficiency, improved propulsion/transmission/drivetrain systems, and improved survivability and crashworthiness through structural design. Solutions have to be found to the hard aerodynamic problems regarding the complex interactions of retreating blade stall effects, advancing blade shock effects, and structural dynamics. The ability to achieve improved rotor performance depends upon an adequate definition of the flow field in which the rotor blades operate and on the design of blades to be more efficient under these conditions. High dynamic rotor loads limit the high-speed and maneuverability capabilities of helicopters. The goal of the rotor technology program are: re-

duction of unstalled high speed pitching moments, stall pitching moment growth, blade bending moments, hub vibratory forces; improvement of aeroelastic stability, with no limit within perfomance flight envelope, no aeromechanical oscillations, and no air resonance limits; better control and stability characteristics; hover figure of merit greater than 0.82, with higher speed capability.

Inflight experimentation of the various components necessary for simple and compound flight modes, and various approaches that avoid the limitations of the retreating blade stall, have been made with some kinds of compound helicopters.

The Rotor System Research Aircraft (RSRA) by the NASA and the United States Army is a program to provide a versatile rotor research facility over a broad range of flight operating conditions, permitting development of promising advanced rotor concepts, figure 1. One RSRA is configurated as a helicopter and another as a compound helicopter. The first one has a design gross weight of 81,740 N. It is powered by the Sikorsky S-61 rotor and drive system with two T58-GE-5 turboshaft engines for the main transmission, the 18.9-meter diameter main rotor, the tail takeoff drive shaft, the intermediate gear box, the tail gear box, and the 3.35-meter diameter tail rotor. The horizontal stabilizer is a "T" tail with a 4.04-meter span and an area of 3.29 m^2. The compound configuration has a gross weight of 116,390 N. Wing and auxiliary thrust jet engines are added to the helicopter, and the tail is changed (adding a 6.86-meter span lower horizontal stabilator [stabilizer-elevator], a rudder, and associated controls; and replacing the helicopter fixed stabilizer with a smaller 2.59-meter span stabilizer). The wing has a 13.72-meter span and includes both aileron and flap surfaces. The wing incidence is variable in flight from - 9° to + 15°. The two auxiliary jet engines are TF - 34 - GE - 400A high-bypass-ratio turbofans with maximum rated static thrust of 41,200 N each. As a compound helicopter, the auxiliary propulsion engines and the variable incidence wing are installed, while in the helicopter configuration these items are removed. The RSRA final configuration is a fixed-wing airplane that provides a fly-back capability should it become necessary to jettison the rotor during compound operation due to a potentially catastrophic operating condition. The RSRA vehicles are designed to meet a recognized need in supplying accurate data for verification and guidance in the further development of rotorcraft technology. The adaptability of the RSRA to new rotor types and concepts will provide a lower cost approach to the high risk development that can cause impulses in the technology trends of rotorcraft.

The Bell XV-15 Tilt Rotor is a concept characterized by an aircraft having three principal flight modes: helicopter, conversion, and airplane, figure 2. This in turn implies that increased research and development efforts may be required to ascertain the possibilities of hybrid rotorcraft to be developed into economic medium and short haul passenger/cargo

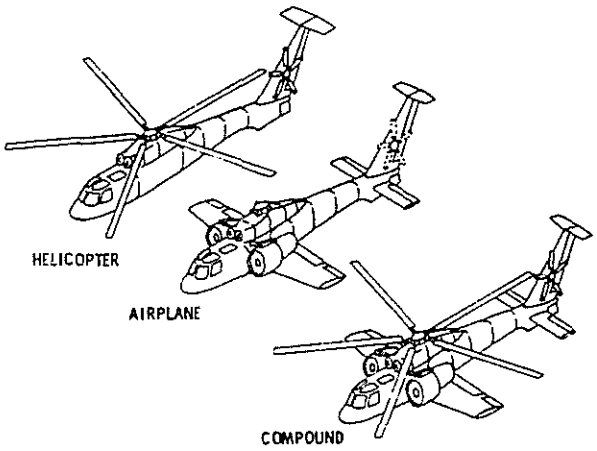

Fig. 1 - RSRA Flight Configuration.

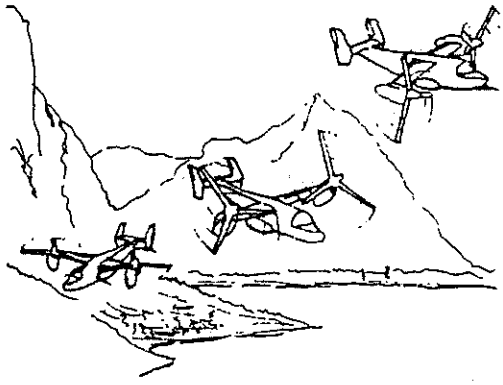

Fig. 2 - Tilt Rotor Principal Flight Modes.

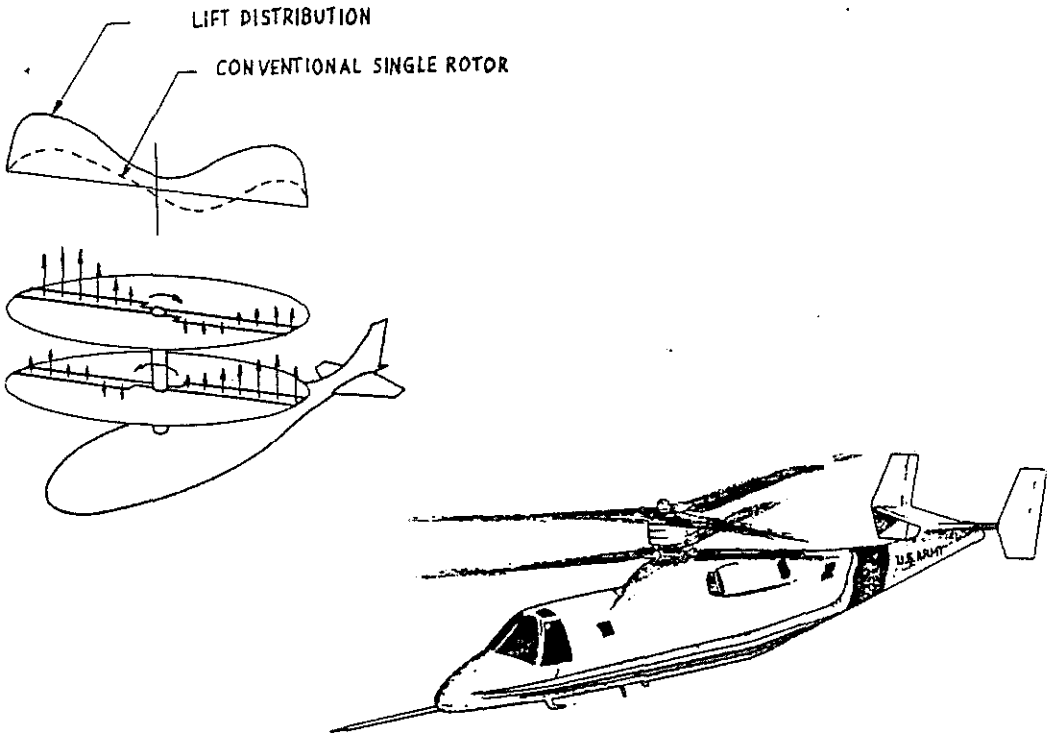

Fig. 3 - XH-59A Advancing Blade Concept, and Lift Distribution.

transports. The tilt rotor aircraft is characterized by two rotors in the horizontal plane, whereas, in forward flight, the rotors act as propellers and all lift is generated by the wing. Maximum speed of 550 km per hour are planned with this vehicle. The aircraft weighs 57,750 N and has a rotor diameter of 7.62 m. The primary advantage of the tilt rotor is that it combines the efficient static lift (hover) capability, normally associated with the low disc loading helicopter, with the efficient cruise performance and low vibration of a fixed wing turboprop aircraft cruising speed of over 550 km/hour. The tilt rotor blade geometry represents a trade-off between the hover and cruise requirements. However, by reducing the rotor tip speed to about 80 percent of the hover value after conversion to the airplane mode, the extent of the compromise is minimized due to increase in blade loading. Therefore, cruise propulsive efficiency is increased while engine performance and engine transmission/drive system torques are maintained at desirable levels.

The Advancing Blade Concept (ABC) by the US Army, figure 3, is a coaxial, counterrotating, hingeless helicopter rotor system. The rotor blades are extremely stiff and are rigidly attached to the rotor hub. Rotor blade pitch is controlled by swashplates in the same manner as conventional rotors. The combined lift distribution over the two 3-bladed rotors is symmetric about the vehicle centerline, and the lift on the advancing blade is not limited by the necessity to balance the stalled retreating blade (forward speed up to 370 km/hour, and 550 km/hour with auxiliary propulsion). Unique to this concept, however, is the ability to intentionally vary the loading on the advancing side of the rotor as compared to the retreating side. This feature, made possible by the stiff and counterrotating, rigidly attached, blades, largely reduces classical retreating blade stall and permits operation at higher thrust coefficients and advance ratios. Further, the stiff blades should be able to operate more easily without aeroelastic instabilities as rotor speed is reduced. Such operation is required for high speed flight, where the advancing blade tip Mach number should not exceed a value of approximately 0.85. Flight gross weight is 49,000 N, and rotor diameter is 11 m. Advantages of this double rotor are: deletion of the requirement for a tail rotor with attendant benefits in safety, simplicity, vulnerability, compactness, noise signature, and performance; high speed capability without wings when provided with a source of horizontal thrust.

The X - wing (stoppable rotor) Aircraft achieves forward flight by a stopped, four-blade lifting rotor used in conjunction with auxiliary propulsion. The configuration currently under investigation, figure 4, utilizes a circulation control airfoil, with blowing from both leading and trailing edges. Active control of the pneumatic system that provides the blowing is required, in order to assure stability during the stopping process at forward speed; also, high stiffness is required to avoid structural divergence of the forward-swept blades. This concept may be applied to high-speed rotorcraft capable speeds up to 750 km/hour.

Several approaches to increasing helicopter speed capability have been tried in the past, and new concepts are currently under development. For them, the utility function is a combination of lifting (high performance in the hover conditions) and transportation (efficient cruise performance). The hover performance is defined as |hover duration in hours · payload weight/gross weight|, and depends on several vehicle parameters including engine specific fuel consumption, structural weight fraction, and mechanical efficiency of the transmission. The cruise performance is defined as |cruise range in kilometers · payload weight/gross weight|, and depends, in addition to the previous factors, on cruise lift-to-drag ratio for the overall configuration and on cruise speed.
These important parameters for the helicopter, the compound helicopter, and the fixed-wing vertical and take off landing aircraft (VTOL) are compared qualitatively in figure 5. The compounds helicopter lies in between the performance extremes of the helicopter and the fixed-wing VTOL, and represents a compromise of hover performance in order to improve velocity and range.

2. UNFEASIBILITY OF DUCTED ROTORS-JETS COMBINATION

The tilt rotor/fixed lifting wing concept, figure 2, and the advancing blade concept, figure 3, represent efficient compromises between the hover and cruise requirements for some kinds of missions.
Both these VTOL capabilities are of course realized in terms of increased complexity and increased empty weight factor, and are obtained through separated turboengines for the rotors and the auxiliary horizontal thrust. Eliminating, as in figure 2, the requirement to operate the rotor in the edgewise flight mode for high speed cruise permits the blades to be tailored with a high spanwise twist and camber distribution that significantly reduces induced and profile losses, therefore improving hover efficiency. From the other hand, such appropriate cruise mode configuration behaves significant drag reduction in as much as avoids the interference drag caused by the lift producing devices. The tilt rotor aircraft operates in the helicopter regime of flight a very small portion of its total operating time, can accelerate from a hover to airplane cruise flight in 30 seconds, has a conversion time of 12 seconds; and the band between the minimum and maximum flight speeds throughout the rotor-mast tilting process is typically greater than 100 km/hour.
Flight results have demonstrated that classical retreating blade stall might be substantially deleyed with a configuration like the advancing blade concept as in figure 3, in which rotor blade pitch is controlled by swashplates in the same manner as conventional rotors. The high-speed capability is achieved without wings when provided with a source of horizontal thrust.

There are certain military and civil missions which appear particu-

larly well suited for the characteristic capabilities of one or the other helicopter compound systems.

It is not possible a compound configuration like the one sketched on figures 6 and 7, in which vertical and horizontal thrust should be obtained through a combination of ducted tilting rotors and jets at their peripheries. In there: compressed air, conducted through the hollow rotor hub and deflected to a radial turbine, should be expanded before entering the two counterrotating nozzle rings, each giving equal torque to high solidity lifting blade rotors; the air leaving the turbine rings should be directed, through fixed radial tubes, to the rotor static outer boundary for a further expansion in tangential tip nozzles to form cold (or warm, by fuel mixing and combustion) jets in the flight direction. For such pneumatic rotor drive, it should be necessary: variable geometry turbocompressor-engines, to change flow rate and compression ratio as needed by flexibility of rotor torque, and overall expansion ratio required in the range of flight conditions from hover to high forward speed; rotor collective (but not cyclic) pitch variability to govern the amount of lift, small rotor tilting in forward flight for maneuvering, and variable geometry and orientation of the thrust nozzles; stator vanes, under the counterrotating rotors, conformed to give everywhere axial flox perpendicular to the rotor planes.
The system of figure 6 and 7 is not feasible because of the small torque obtainable from a small diameter radial turbine. In fact, figure 8, torque M and weight flow Q corresponding to a useful power P = 1,100 kW are (with $\eta_c = 0.85$, $\eta_t = 0.8$, $p_2/p_1 = 10$)

$$Q = \eta_c \, P/c_p \, T_1 \left| (p_2/p_1)^{\frac{k-1}{k}} - 1 \right| = 33.24 \text{ N/s}$$

$$M = M_1 = M_2 = \eta_t \, P \cdot 1{,}000/2\omega = 5{,}283 \text{ Nm} =$$

$$= Q \, (c_3 \cos \alpha_3 \, r_3 + c_4 \cos \alpha_4 \, r_4)/g = M_1$$

$$= Q \, (c_5 \cos \alpha_5 \, r_5 + c_6 \cos \alpha_6 \, r_6)/g = M_2$$

for a rotor with R = 3 m and tip speed V_t = 250 m/s (rotor speed N = 795 rpm). Because of the small values of the weight flow Q and the absolute velocities c_3 and c_4 (maximum theoretical value for the impulse turbine $c = \sqrt{2g \; 1{,}000 \; c_p \; T_2 \left| 1 - (p_1/p_2)^{(k-1)/k} \right|} = 1{,}230$ m/s), the torque M_1 = = 5,282 Nm might be obtained at too high radii (more than the fixed value of the rotor radius) of the corresponding first stage impulse turbine, and the torque M_2 = 5,282 Nm should require still higher radii and a se-

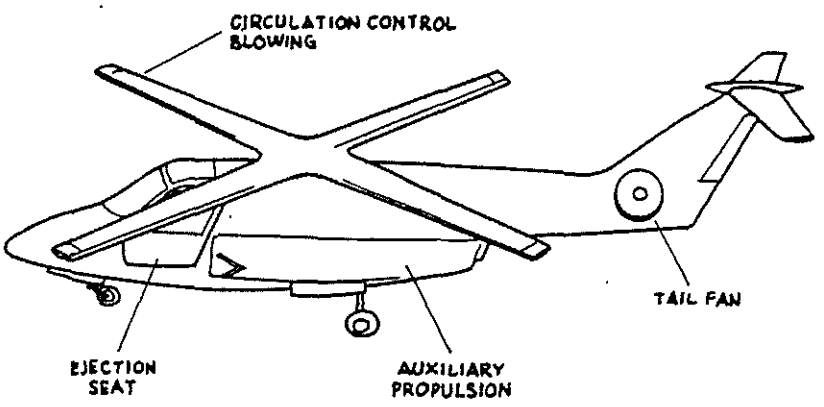

Fig. 4 - X-Wing Aircraft.

	HELICOPTER	COMPOUND ROTORCRAFT	FIXED WING VTOL
$\frac{L}{D}_{HOVER}$	HIGH	MEDIUM	(LOW)
SPEED	(LOW)	MEDIUM	HIGH
$\frac{L}{D}_{CRUISE}$	(LOW)	MEDIUM	HIGH
PAYLOAD FRACTION	MEDIUM	(LOW)	(LOW)
HOVER PERFORMANCE, hours	1 TO 2	0.5 TO 1	0.05 TO 0.1
CRUISE PERFORMANCE, n. mi.	50 TO 150	100 TO 200	150 TO 200

Fig. 5 - Characteristics of Rotorcraft.

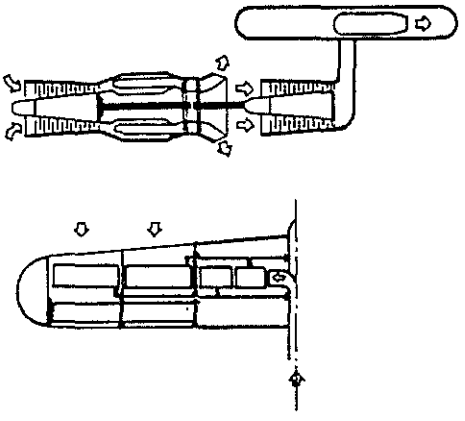

Fig. 6 - Ducted Rotors Jets Combinations.

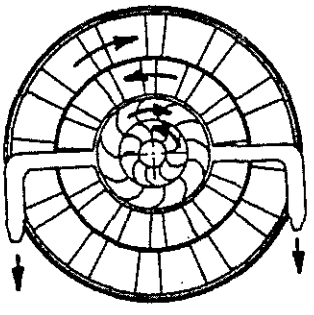

Fig. 7 - Radial Distribution of Ducted Rotors - Jets Combination.

cond impulse stage turbine (reaction turbine being impossible because of the large interested cross sectional area).

The only possible solution for driving the ducted counterrotating high solidity rotors is therefore the turboshaft engine, as on figure 9. In respect to advancing blade concept of figure 3, the retreating rotor blade stall is completely avoided, and the rotor diameters are quite smaller than usually because of the higher specific axial thrust; but the increased aerodynamic drag of the ducted rotors limits the cruise speed. In respect to the tilt rotor concept of figure 2, the compound configuration of figure 9 has the advantage of increased hover efficiency because of rotor blades with higher spanwise twist. But there is significant drag increase during cruise flight because of the interference drag caused by the lifting producing devices, and because of aerodynamic drag of the ducts around the rotors. Stator vanes, under the counterrotating rotors are necessary to have everywhere axial flow perpendicular to the rotor plane. Forward flight is made possible only by auxialiary propelled mode using two turbojets.

3. AERODYNAMICS OF SINGLE AND DUCTED COMPOSITE COUNTERROTATING ROTORS

Hovering and vertical flight performance analysis

On the assumption that a single rotor has an infinite number of blades and that no swirl is imparted to the flow, the thrust T by a frictionless fluid should be uniformly distributed, requiring the power P, as the expressions, Ref. 1

$$T = 2\pi R^2 (V + v) \rho v \qquad (1)$$

$$P = T (V + v)/1{,}000 \qquad (2)$$

(with V and v, respectively, the rate of climbing and the induced velocity). In particular, in hovering flight at sea level

$$v = 0.64 \sqrt{T/\pi R^2} = 0.64 \sqrt{D.L.}$$

It follows that the disc loading D.L. = $T/\pi R^2$ should be kept as low as possible for efficiency hovering performance.
For making preliminary estimates of actual helicopter hovering performance, the rotor figure of merit (with P corresponding to the actual total power) Q = Tv/1,000 P = P.L. $\sqrt{D.L./2\rho} = c_T^{3/2}/c_M \sqrt{2}$ is compared with the

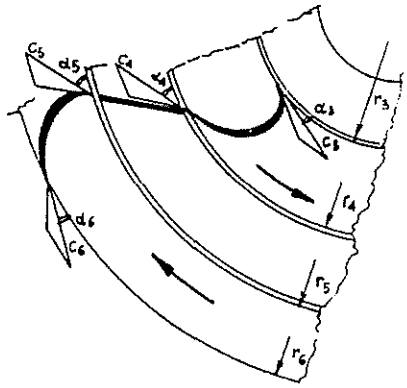

Fig. 8 -
Radial Turbines For Counterrotating Blade Rings.

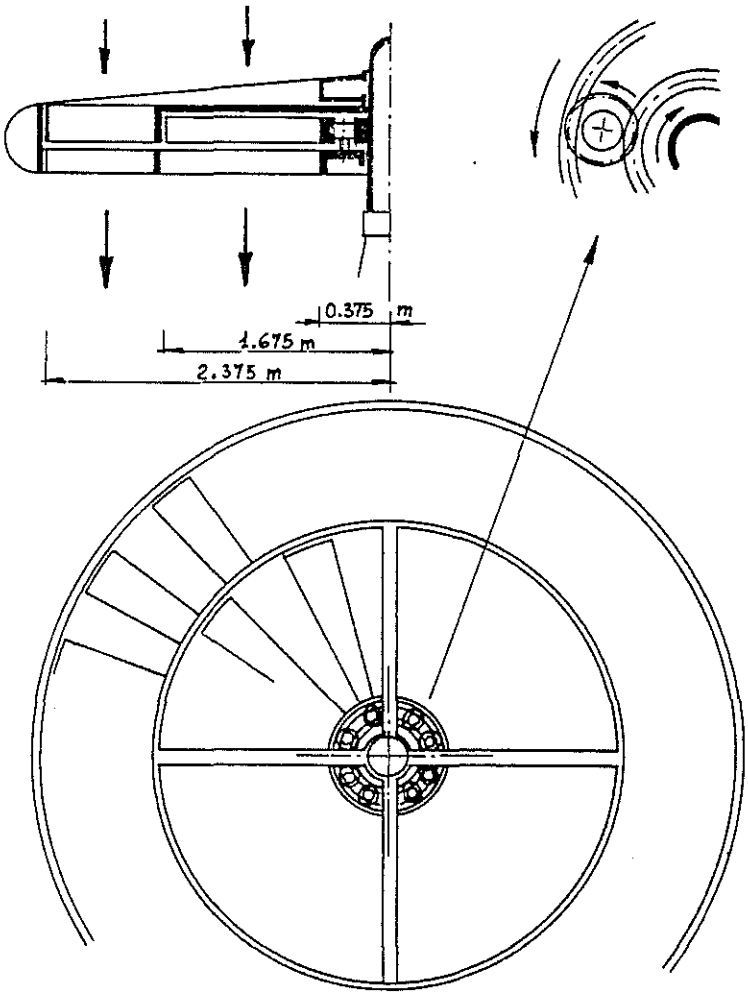

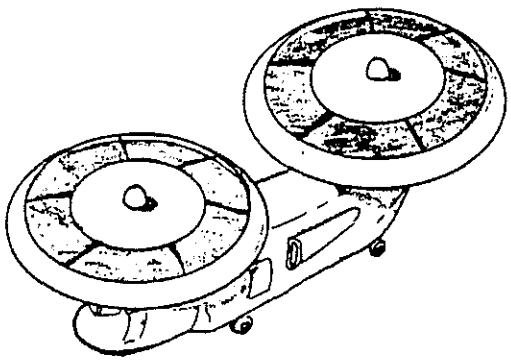

Fig. 9 -
Solution for High Altitude Ducted Counterrotating High Solidity Rotors.

disc loading and the power loading P.L. = T/1,000 P, as on figure 10 at sea level conditions. An actual single rotor requires a total power, to hover with a given load, in which about 60%, 30%, 0.5% and 3.5% is required, respectively, for induced power T v (minimum possible power requirement to hover), profile drag losses, nonuniform inflow, slipstream rotation, and tip losses. Flutter of the blades, transient effects due to the interaction of the tip - vortex of one blade with a following blade and wake induced instabilities, are unsteady aerodynamics losses in there considered.

Eqs. (1) and (2) do not provide information as to how the rotor blades should be designed so as to produce a given thrust, and ignore profile - drag losses. Considering the forces acting on each blade element of the rotor in the helical path of the climb condition, figure 11, the effects of profile drag, rotor tip speed and solidity, on figure of merit Q may be expressed, Ref. 2, for constant blade chord, pitch angle linearly variable with the radius, and b blades, as in figures 12 and 13

$$T = c_T \pi R^2 \rho \omega^2 R^2 \tag{3}$$

$$c_T = \frac{a}{4} \frac{bc}{\pi R} (\theta_t - \phi_t) = \frac{\sigma}{4} a (\theta_t - \phi_t) \tag{4}$$

$$M = c_M \pi R^3 \omega^2 R^2 = \frac{b}{4} \rho \omega^2 R^4 c \left|\frac{\partial}{2} + a \phi_t (\theta_t - \phi_t)\right| \tag{5}$$

$$c_M = \frac{\sigma}{4} \left|\frac{\partial}{2} + a \phi_t (\theta_t - \phi_t)\right| = \frac{c_T^{3/2}}{\sqrt{2}} + \frac{a\partial}{8} \tag{6}$$

$$Q = \frac{1}{\sqrt{2}} c_T^{3/2} / (c_T^{3/2}/\sqrt{2} + a\partial/8) \tag{7}$$

$$\bar{c}_L = 6 c_T/\sigma \tag{8}$$

where c, b, θ_t, ϕ_t, σ, ∂, $\bar{c}_L$ and a, are, respectively, blade chord, number of blades, pitch and inflow angles of the blade tip, solidity, average blade profile - drag coefficient, mean lift coefficient, and the lift slope

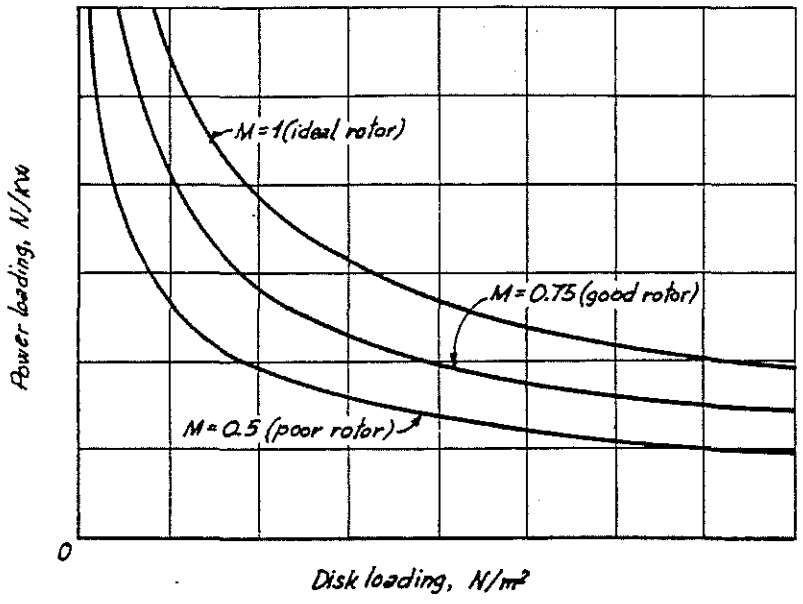

Fig. 10 -
Rotor Power-loading
against Disk-loading.

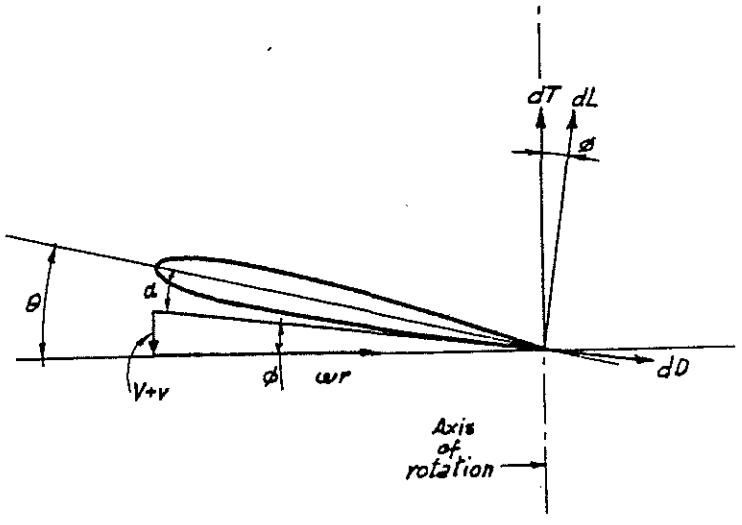

Fig. 11-
Rotor Blade Element.

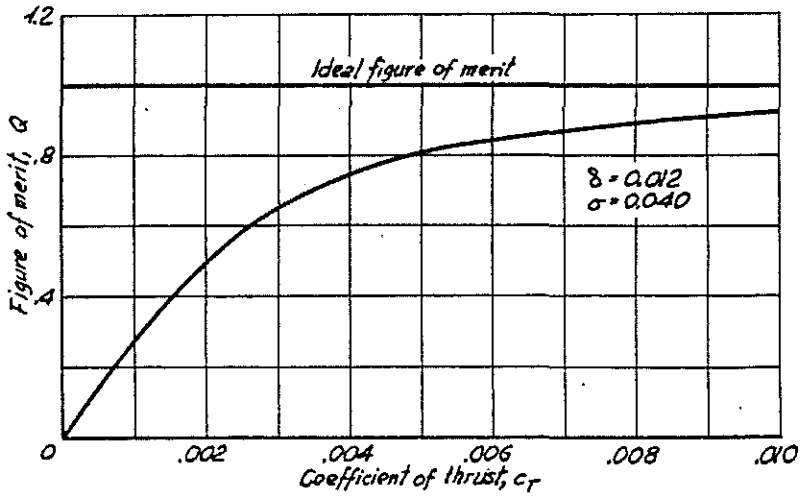

Fig. 12 - Figure of Merit against Thrust Coefficient.

of the section $|a\alpha = a\ (\theta - \phi)$ being the lift coefficient|.

The static thrust case has very few design methods which allow predictions of detailed loading distribution to be made. Accuracy in calculation of VTOL rotor performance requires, however, to be emphasized by noting that a 1 percent change in the lifting capability of a rotor, at a given power input, may mean a 10% change in payload for the aircraft, and perhaps the difference between profitable and unprofitable flight operation. A complete analitical prediction would also allow for an optimization of the blade geometry and operating conditions at a given mission requirement.
The introduction of smoke into the flow, with stroboscopic lighting, has provided visualization of the region near the rotor to see completely the contraction of the wake and other distortion, with a blade loading not conform to the ideal distribution. It results that the wake from a blade consists of a strong tip vortex and an inner vortex sheet of opposite sense, figure 14. The outer part of the sheet moves faster than the inner part, with the consequence that the sheet becomes more and more inclined to the rotor plane; the outer part of the sheets moves faster than the tip vortex. Tip and inner sheet vortices interfere in a multi-blade rotor.

Accurate determination of the thrust produced and the power required by the rotor is necessary for a precise estimation of helicopter performance, taking into account the physical design of the rotor blades. For that, the induced velocity v on b generic blade elements $c \cdot dr$ distant r (adimensionally $x = r/R$) from the rotor shaft may be obtained equating the differential thrusts derived by eqs. (1) and (3) - (4). Once the induced velocity is known, the inflow angle $\phi = (v + V)/\omega R\, x$ may be found. Inflow, pitch and attack, angles become, for ideally twisted blades, $\phi_x = \phi_t/x$, $\theta_x = \theta_t/x$ and $\alpha_x = (\theta_t - \phi_t)/x$. But, uniform inflow distribution requires a different twist for each thrust coefficient c_T.
The experimental data (assuming no tip losses) are shown on figure 15, Ref. 3, compared with theoretical values of v calculated as above mentioned.

General performance equations in hovering for the charcteristics of rotors having arbitrary plan forms and airfoil sections in non-uniform inflow distribution, neglecting tip losses, depend upon the local values of σ_x, ϕ_x (resulting from the induced velocity for $V = 0$) and α_x, that determine local thrust and torque expressed in coefficient form, Ref. 2

$$d\, c_T/dx = \sigma_x\, a\, \alpha_x\, x^2/2 \qquad (9)$$

$$d\, c_M/dx = \sigma_x (a\, \phi_x\, \alpha_x + c_d)\, x^3/2 \qquad (10)$$

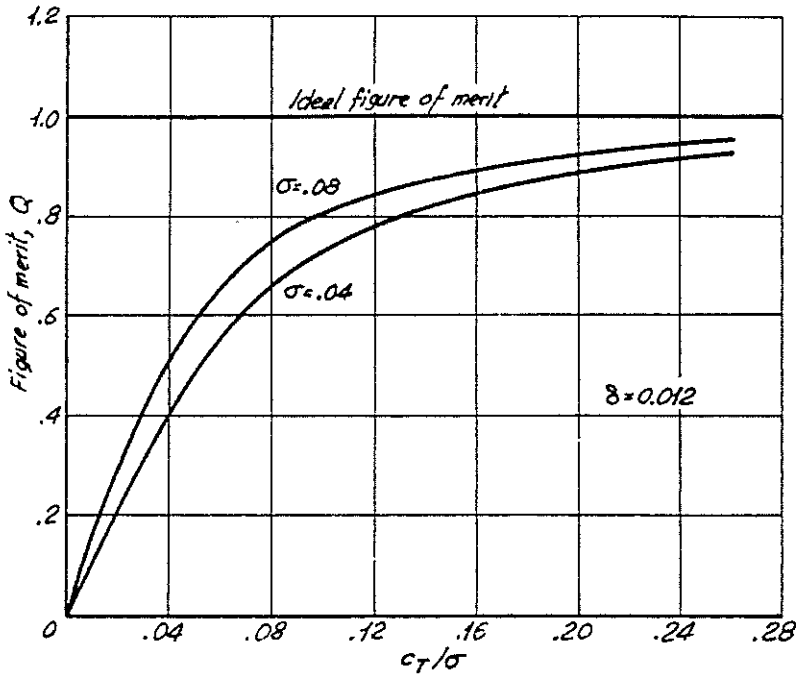

Fig. 13 -
Figure of Merit versus
Thrust Coefficient
Solidity Ratio.

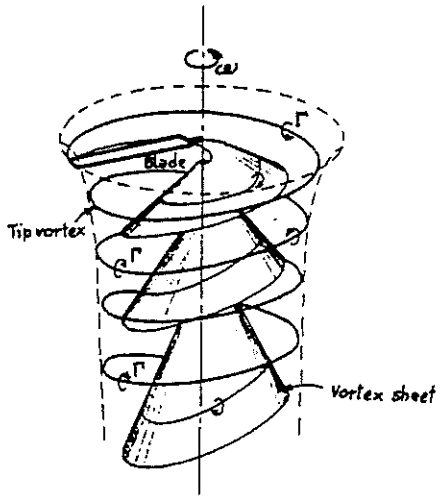

Fig. 14 -
Wake Velocity in Hovering Flight.

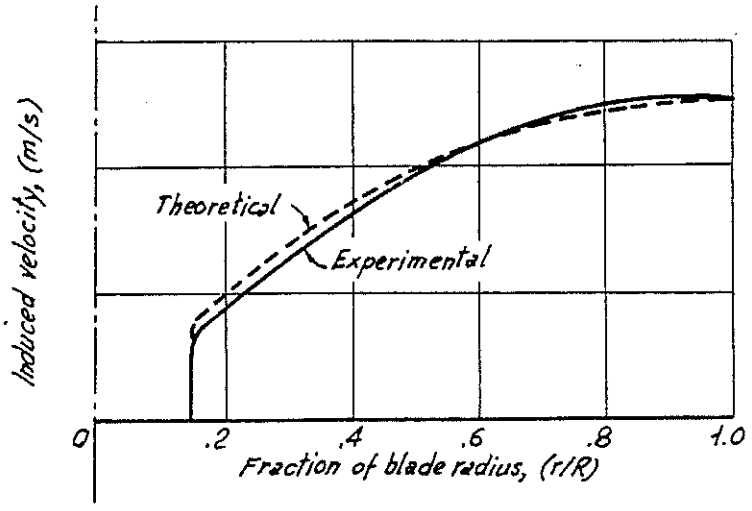

Fig. 15 - Induced Velocity in Single Rotor.

(considering for c_M the induced and profile - drag contributions; c_d being the section profile - drag coefficient).
For calculating the absolute performance of the rotor, a factor that takes into account the reduction in thrust near the blade tips resulting through the use of a finite number of blades, in the form $B = 1 - \sqrt{2}\, c_T / 2$, Ref.4, has to be introduced. Effects of blade twist, taper and climb, on induced power loss influence operating conditions.
The proximity of the helical wake is a contributing factor to blade flutter in hovering flight. In fact, when the rotor has high inflow through the disc, the wake of a blade is removed rapidly away as indicated in figure 16a and its effect on the aerodynamic forces on the blade is approximately the same as that of a rectilinear wake. For the case of low inflow the wake is closely coiled under the rotor disc as illustrated in figure 16b and it can have a strong influcence on the aerodynamic forces acting on a blade at certain frequencies of blade oscillation.
Figure 17 and 18, Ref. 5, show, for example, the thrust and power distribution on a three blade rotor for geometry angles $\theta = 12°$ and $14°$ at $x = 0.75$. The blade chord has been assumed to be zero at the tip to force values of thrust and power to be zero there. Integrated values of thrust and power coefficients and figure of merit, as directly measured, are, for $\theta = 12°$ and $14°$ respectively, $c_T = 0.1565 - 0.1815$, $c_P = 0.06 - 0.07$, $Q = 0.823 - 0.817$.
In figure 19, Ref. 2, the manner in which twist affects the inflow distribution and the blade loading (as represented by the section angle of attack) of an untapered blade operating at a representative $c_T = 0.0056$ and $\sigma = 0.06$. It appears that the maximum blade loading is higher near the inboard end of the blade, expecially at ideal twist, with the consequence to minimize the blade stall.

The induced velocity v_c produced by a rotor in the climb condition is less than in hovering, in as much as the rotor handles a greater mass of air and consequently needs to accelerate the mass less to produce the same thrust. Instead of $v = \sqrt{T/2\rho\pi R^2}\sqrt{c_T/2}$ obtainable from Eq. 1 relative to an ideal rotor, the induced velocity in climb becomes

$$v_c = (-V + \sqrt{V^2 + 4\, v^2})/2 = (-V + \sqrt{V^2 + 2\, c_T\, \omega^2\, R^2})/2 \qquad (11)$$

The actual power required in climb P_c is, however, less than $P + W\ V/1{,}000$ deduced with no changes in the induced or profile - drag power losses resulting from the climb velocity. The increase in respect to the hovering power P is in general approximately half the rate of change of potential energy of the helicopter, because of the corresponding increase in lifting efficiency.

In the coaxial helicopter, fuselage torque is eliminated by utiliz-

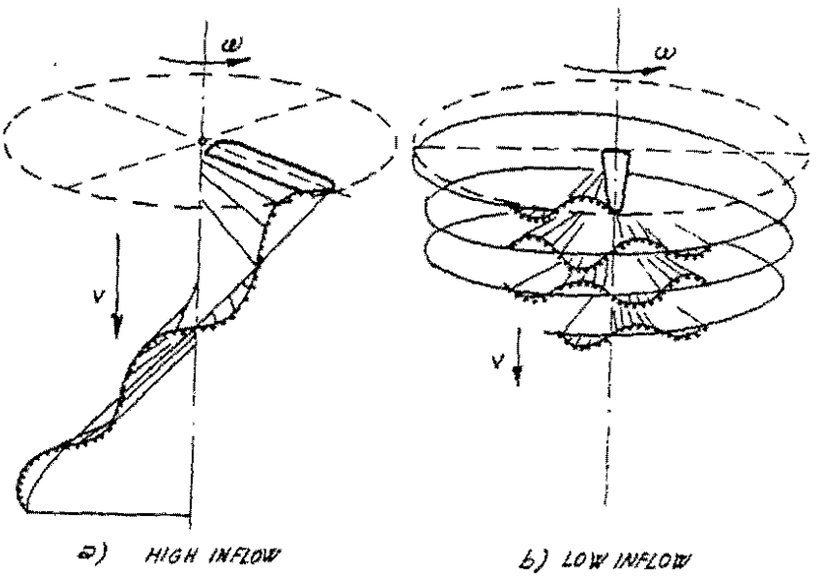

Fig. 16 - Unsteady Rotor Flow Field.

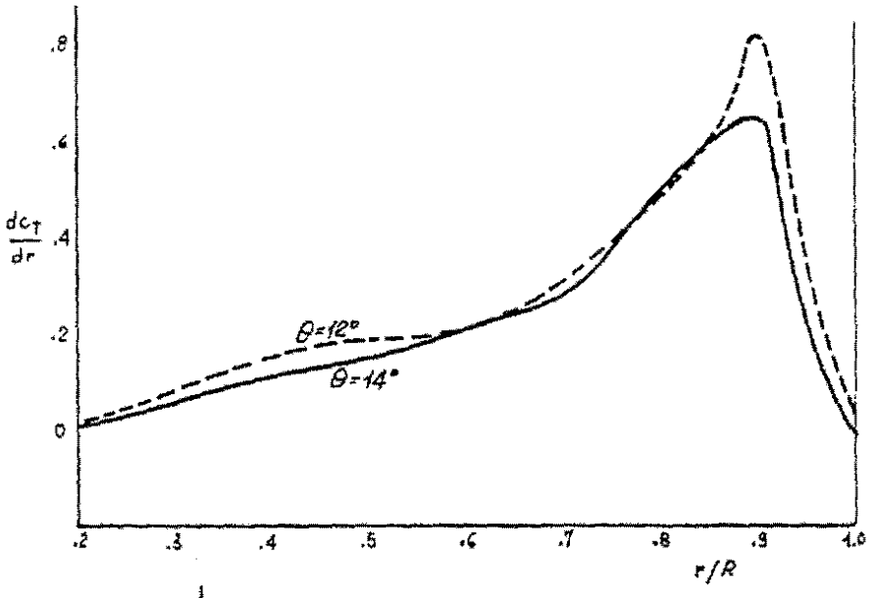

Fig. 17 - Thrust Distribution.

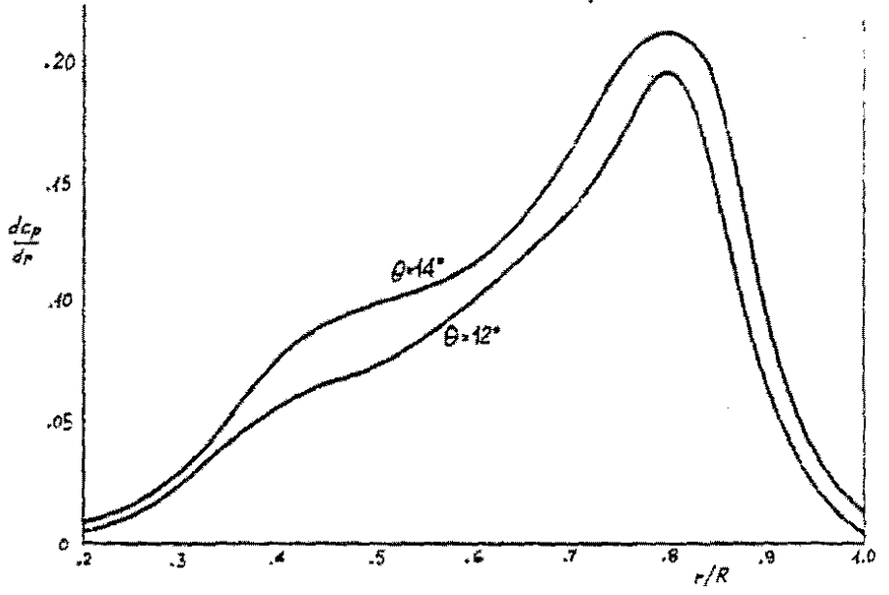

Fig. 18 - Power Distribution.

ing two superimposed rotors, rotating in opposite directions and abs ing the same torque. The advantages are those of having overall dimen sions defined only by the rotor diameter, and of a saving of power ov the single rotor - tail rotor design.
The flow from the two rotors in series is meanly axial, both outgoing the first and the second ones, even though the high radial velocities along the twisted blades determine the vortices shown on figure 14. T superimposition of two series of counterrotating vortices has the eff to improve the aircraft and rotor figure of merit.

For instance, the ABC coaxial counterrotating, hingeless helic ter rotor system of figure 3, with blades extremely stiff and rigidly attached to the rotor hub, has reached, in the first flight (1976) of XH - 59A prototype, the aircraft figure of merit $Q_A = 0.647 = (P.L.)_A \cdot \sqrt{D.L./2\rho}$, in which $(P.L.)_A = W_{max}/1{,}000\ P = 48{,}865/1{,}000 \cdot 1{,}100 = 0.$ and $D.L. = W_{max}/\pi R^2 = 48{,}865/\pi \cdot (5.485)^2 = 517\ N/m^2$. Other XH - 59A c acteristic parameters are as it follows: gross weight coefficient $c_W = W_{max}/\pi R^2 \rho \omega^2 R^2 =$ (with $\omega = V_t/R = 198.1/5.485 = 36.1$ rad/s $= \pi N = \pi\ 345/30$); power coefficient $c_P = 1{,}000\ P/\pi R^2 \rho \omega^3 R^3 = 0.00123$; th coefficient $c_T = T/\pi R^2 \rho \omega^2 R^2 = 0.0108$; rotor solidity $\sigma = 0.127$; c $= 0.085$.

As comparison, the aircraft figure of merit of the US Utility tical Transport Aircraft System (UTTAS) and Advanced Attack Helicopte (AAH) are, respectively: UTTAS, $Q_A = 0.388$, because of $(P.L.)_A = 73,($ $/1{,}000 \cdot 2{,}270 = 0.0322$ and $D.L. = 73{,}078/\pi \cdot (8.18)^2\ 348\ N/m^2$, (othe parameters being, 4 blades, chord 0.53 m, $\sigma = 0.0826$, N = 258 rpm, σ rad/s, $c_P = 0.00082$, $c_T = 0.00584$, $c_T/\sigma = 0.0708$); AAH, $Q_A = 0.33$, be of $(P.L.)_A = 61{,}416/1{,}000 \cdot 2{,}270 = 0.027$ and $D.L. = 61{,}416/\pi \cdot (7.3$ $= 365\ N/m^2$, (other parameters being, 4 blades, chord 0.53 m, $\sigma = 0.($ N = 289 rpm, $\omega = 30.25$ rad/s, $c_P = 0.001$, $c_T = 0.0061$, $c_T/\sigma = 0.0663$).

The ABC rotor figure of merit, being $T_{max} \simeq 55{,}400$ N ($\simeq 13.4\%$ mc than W_{max}), is $Q_R = T_{max} \sqrt{T_{max}/\pi R^2} \cdot \rho/1{,}000 \cdot P\sqrt{2} = 0.78$. In fact, a method of presenting isolated rotor hover performance is to show rotor figure of merit Q_R plotted against blade loading c_T/σ, as in the prelin nary XH - 59A design estimate, shown on figure 20. Ref. 6.
Figure 21 shows the XH - 59A aircraft figure of merit (Q_A) compared tc other US Army helicopter figures of merit. However the most obvious re: sons for the high Q_A of the XH - 59A aircraft is symply that there is tail rotor to power, which normally accounts for 8 to 10 percent of power.

The ducted composite counterrotating rotor system of figure 9 averagely realizing in the external (2) and in the internal (1) roto rings, respectively, the velocity diagrams of figure 22.
Referring to the flight gross weight W_{max} and the power P of the ABC icopter, the stator vanes configuration is establihed in order to get

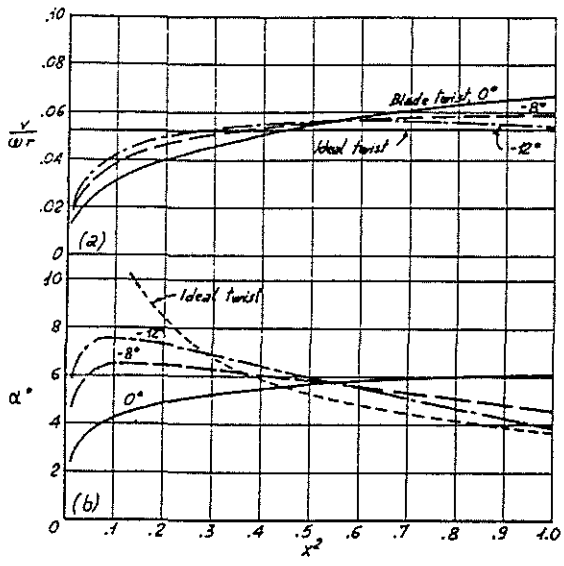

Fig. 19 -
Induced Velocity and Angle of Attack in Hovering.

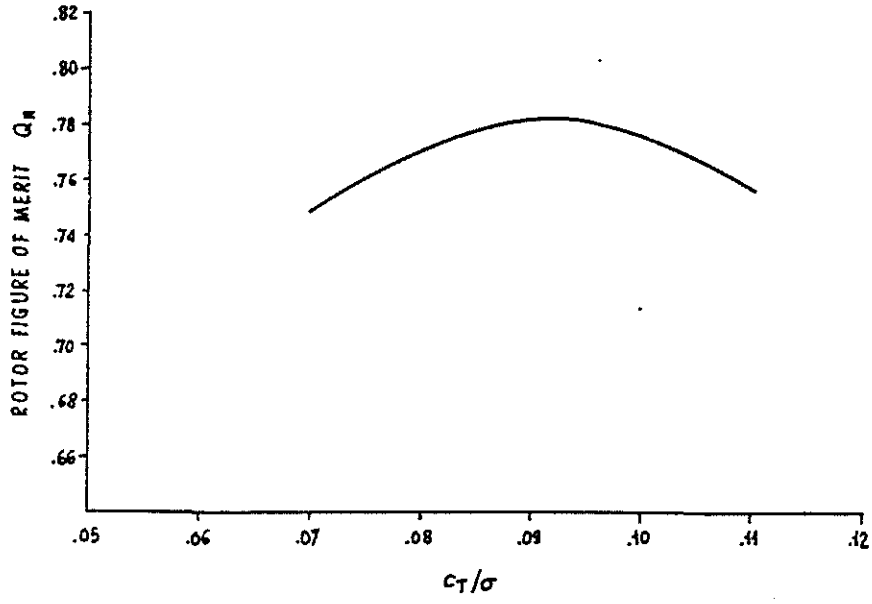

Fig. 20 - XH - 59A Advanced Blade Concept, Rotor Figure of Merit.

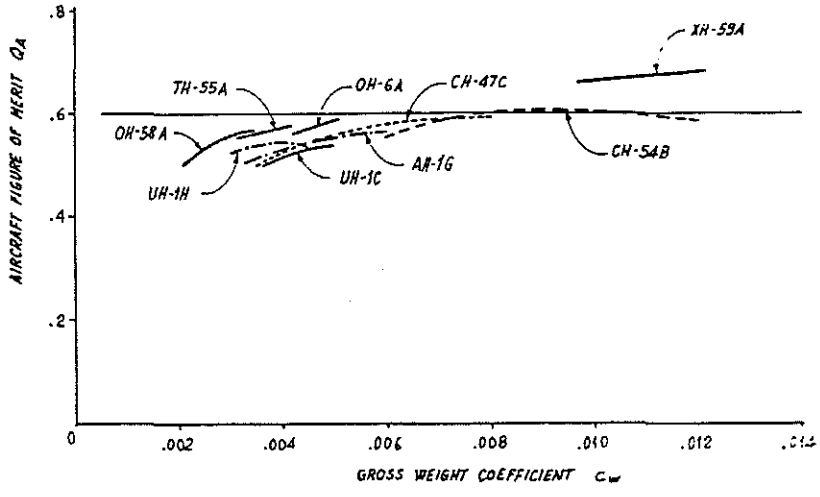

Fig. 21 - Helicopter Figure of Merit Trends.

stant (along the radius) and axial induced velocity v at the exit. It is therefore, in hovering with a predicted value $Q_A = 0.82$ for the aircraft figure of merit,

$$v = 1{,}000\ P\ Q_A/T = 1{,}000 \cdot 1{,}100 \cdot 0.82/48{,}865 = 18.45\ m/s$$

$$M_1 = M_2 = M/2 = 1{,}000\ P/2\omega = 1{,}000 \cdot 1{,}100/2 \cdot 36.1 = 15{,}235.5\ Nm$$

Because of the high solidity σ_x in both the rotor rings, the relative velocities acting on the blade airfoil at the radius r are separated by a peripheral component $(\Delta W)_x$, whose values is obtained from

$$v \cdot t \cdot dr \cdot \rho\ (\Delta w)_x = dL\ \sin\theta + dD\ \cos\theta$$

as

$$(\Delta w)_x = \frac{v \cdot \sigma_x \cdot c_{Lx}}{2 \sin \theta_t/x}\ (1 + c_{Dx} \cdot \operatorname{ctg} \theta/c_{Lx}) \qquad (12)$$

The torques are approximately

- external rotor ring and its driving 4 blade rotor (Eq. 5)

$$M_2 = 2\pi v\rho \int_{R_1}^{R_2} (\Delta w)_x r^2\ dr + b\rho\omega^2\ R_1^4\ c\ \left|\frac{\partial}{2} + a\ \phi_t(\Theta_t - \phi_t)\right| \qquad (13)$$

- internal rotor ring

$$M_1 = 2\ \pi\ v\ \rho \int_{R_0}^{R_1} (\Delta w)_x r^2\ dr \qquad (14)$$

The force balance in the axial direction corresponds, in hovering, Eq. 4, to

$$b\int_{R_0}^{R_2} (dL \cdot \cos\frac{\theta_t}{x} - b\int_{R_0}^{R_2} dD \cdot \sin\frac{\theta_t}{x} + \frac{\sigma}{4}\ a(\theta_t - \phi_t)\ \pi\rho\omega^2\ R_1^2 =$$

$$= W_{max} + \frac{1}{2}\rho\ v^2\ \pi(R_2 - R_Q) \qquad (15)$$

From Eqs. (13), (14) and (15), the radii R_1 and R_2 and the rotor configuration may be deduced.

Forward flight performance analysis

The ABC XH-59A coaxial, counterrotating, helicopter rotor system performs a ratio L/D = 4 (sea level standard) at V_F = 225 km/h calibrated speed. Figure 23 shows how this value compares with other US Army helicopters; lift/drag (L/D) ratios shown in this figure are calculated at speed for best range and represent various configurations, gross weight, and altitudes.
The flapping angle, for D/L = 1/4 = tan α(V_F = 225 km/h), and the helicopter drag are, respectively α = 14° and D = 48,865/4 = 12, 216 N.
The design speed of the hingeless rotor system was 250 to 300 km/h in the basic helicopter configuration, and up to 550 km/h in the auxiliary propelled mode using two turbojets to provide an additional maximum horizontal thrust of 25,765 N.
The XH-59H prototype has zero degree fixed tilt, considered to be the best compromise between conventional helicopter speed requirements and high-speed requirements with auxiliary propulsion. The maneuver and structural objectives include the ability to achieve sustained load factors of 2.5 g, Ref.s 7 and 8, in the speed range of 130 to 315 km/h with satisfactory maneuvering stability and stress levels.

Now, in a ducted rotor, as in figure 9, very low speed forward flight and maneuvering is possible by tilting a few degree the rotor shaft; and the induced velocity is still giving the required lift through an increased collective angle of attack.

But, transition from low to high speed forward flight requires auxiliary propulsion and inlet and exhaust vanes with variable geometry and composite structure for addressing the rotor inflow in such a way to avoid different lift condition for the advancing and retreating blade. Moreover, the outflow is showing a lift loss as function of the ratio of the forward speed to the rotor exit velocity, accompanied by pitching moment changes whose magnitudes may be such as to give rise to stability problems. The outflow leading to interference effects with the cross flow arising from the forward speed is no complex that there seems little prospect of developing methods for prediction. It should be noted that the lift losses are strongly dependent on aircraft and flow geometries and on the ratio of the forward speed to the rotor exit velocity. When an outflow issues into a cross-flow, it is deflected downstream and its boundaries spread as a result of turbulent mixing in much the same way as occurs with an outflow issuing into still air.
However, when the densities and temperatures of the mainstream and outgoing flow are quite similar, and stator vanes under the rotor are addressing axially the flow, the lift losses are not large even at high forward speed, and may be compensated increasing the blade collective

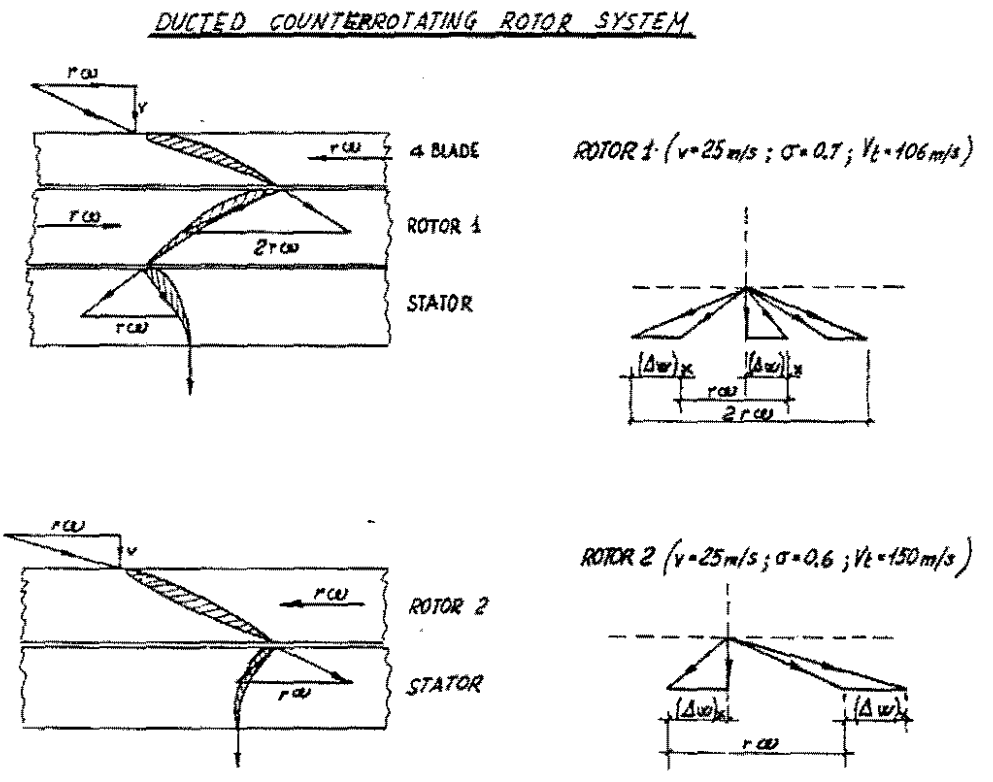

Fig. 22 - Flow Velocity Diagrams in the Counterrotating Rotor System of Figure 9.

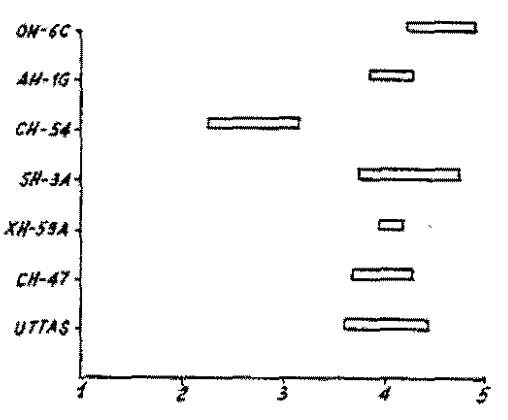

Fig. 23 - Total Aircraft Lift/Drag.

pitch angle.

Eliminating the requirement to operate the rotor in the edgewise flight mode for high speed cruise permits the blades to be tailored with a high spanwise twist and camber distribution that significant reduces induced and profile losses, therefore improving lift efficiency.
The relatively short duration of forward flight in the conventional helicopter mode results in a favorable fatigue environment. The conversion band between the minimum and maximum flight speeds is broad; it requires variable geometry stator vanes for feeding the rotor rings in a way to limit reverse flow in the retreating blades. Furthermore, the conversion has to be stopped or reversed, or the aircraft has to be flown in steady-state at any point in the conversion corridor. The transition from hovering to high speed forward flight will need the flow to supply the rotor axially (through the rotor cross sectional area). Even though the induced velocity at high forward speed is low, the pressure jump in the rotor/stator configuration, because of appropriate blade collective and cyclic pitch control, permits the desired thrust T to be established in order to balance the aircraft weight.
The configuration of figure 9 may be considered in between the rotorcraft classes having, respectively, very low disk loading (as the ABC of figure 3, the RSRA and the tilt-proprotor configuration of figure 2) and high disk loading (as several complex STOL and V/STOL aircraft, including externally blown flap, upper-surface blown flap, internally blown jet flap, and lift jet lift-cruise).

The lift producing devices of the wingless aircraft are two ducted counterrotating rotors. During hover and horizontal forward flight, they have to generate vertical thrust for balancing the aircraft weight. In order to do that, the vertical component of the induced velocity v has to be increased when the weight flow is diminishing and the interference drag due to the forward flight is higher. This is possible because the jump of pressure

$$\Delta p = \rho \cdot (\Delta x)_x \cdot r\omega \qquad (16)$$

generating the induced velocity is depending (12) upon the amount of lift generated by pitching contemporarely all the blades. However, the main advantage of such propulsion system is represented by the possibility to fly at much higher altitudes than present rotorcraft, even though more power is needed (besides, the drag of the ducted rotors during forward flight).

The study of dynamic stability and control of this new kind of wingless VTOL aircraft may seem very complicated, since each ducted rotor possesses degrees of freedom in addition to those of the conventional air-

craft configuration. However, simplifying assumptions derive from the following considerations:

- accelerations of the aircraft are small enough to have a negligible effect on the rotor response;
- the rotor speed is decreasing proportionally to the torque increase required by the generated lift;
- lateral and longitudinal motions are uncoupled and can be treated independently of one another, as is normally the case with the fixed-wing aircraft;
- forward flight is about only produced by the auxiliary turbojet propulsion, while stator inlet variable geometry is permitting the needed lifting thrust;
- conversion time from hover to cruise forward flight should be lengthened to several minutes as dictated by stability problems consequent to the rotor inlet largely variable geometry.

4. DESIGN EVALUATION OF A HIGH ALTITUDE DUCTED ROTOR FOR WINGLESS AIRCRAFT

Considering the gross weight 48,865 N of the ABC XH-59A and the aircraft figure of merit 0.82, an average vertical component $v = 25$ m/s of the induced velocity behaves, at sea level hovering, two ducted rotors of radius ($\xi = 0.9$) .

$$R_2 = \sqrt{48{,}865/\xi\ 4\ \pi(25)^2\ \rho} = 2.375 \text{ m}$$

in which unappropriate change of blade angle of attack should have to generate, at altitude 5,000 m, a velocity $v = 32$ m/s for balancing the weight.

The required power for each rotor is about

$$P = W\ v/2{,}000 \cdot 0{,}82 = 745 \text{ kW} \quad (953 \text{ kW at } 5{,}000 \text{ m})$$

With $V_t = 150$ m/s, $\omega = 63.2$ rad/s and $N = 603$ rpm, the sea level torque for driving a rotor blade ring is

$$M_1 = M_2 = 1{,}000 \cdot P/2\omega = 5{,}900 \text{ Nm} \quad (7{,}540 \text{ Nm at } 5{,}000 \text{ m})$$

For the internal ring, it is possible at sea level an average approximate value $\Delta w_1 = 34.5$ m/s (with $\sigma_1 = 0.7$, $c_{Lx} = 0.7$ and $\theta_1 = 10°$), which requires (Eq. 14) $R_1 = 1.675$ m ($R_o = 0.375$ m) to give $M_1 = 5{,}900$ Nm.
From Eq. 13 (with $\Delta w_2 = 29.7$ m/s, $\sigma_2 = 0.6$, $c_{Lx} = 0.55$, $\theta_2 = 8°$, $b = 4$, $c = 0.15$ and $|\partial/2 + a\,\phi_t(\theta_t - \phi_t)| = 0.02167$), the same torque value 5,900 Nm is obtained with $R_2 = 2.375$ m, figure 9.

In forward flight, the jump of pressure in the ducted rotor - stator, and the air speed higher on the superior part of the disc, act in favour of a lifting surface, largely compensating the distortion of the stator outflow caused by the relative motion. The reverse flow due to the retreating blades may be considered negligible for forward flight up to 100 m/s.

5. CONCLUSIONS

Ducted counterrotating rotors, with their high figure of merit and induced velocity, may be applied to wingless helicopters to balance entirely the weight in hovering and forward flight.

The relative aircraft solution, figure 9, is suitable for missions to altitudes much higher than conventional helicopters; a forward velocity being possible up to 100 m/s by auxiliary propulsion. Tilting the rotors a few degree, a limited manuevering capability is made possible. Variable geometry of the stator vanes under the counterrotating rotors permits to control the outflow during the flight, limiting reverse flow in the retreating blades. The configuration is to be considered in between the low and high disk loading classes; and because of that the rotor diameters are quite less than usually.

Rotor aerodynamic design is facilitated by a better control of the flow, because of the very high ratio of the total blade area to the rotor disk area and the variable geometry. The calculation of the loading of the rotor blades is facilitated by the knowledge of the air induced velocity at any station along the blade.

LIST OF SYMBOLS

M = rotor torque, Nm
Q = weight air flow, N/s; figure of merit
P = power, kW
η = efficiency
c_p = constant pressure specific heat, kJ/NK
T = absolute temperature, K; thrust, N
p = pressure, kPa/m^2
k = specific heat ratio
ω = rotor angular velocity, rad/s

c = absolute velocity, m/s
r = radial position, m
R = main rotor radius, m
g = gravity acceleration, m/s^2
V = velocity, m/s
N = rotor rpm
W = weight, N
v = rotor induced velocity, m/s
ρ = density, Ns^2/m^4
c_T = thrust coefficient, $T = c_T \pi R^2 \rho(\omega R)^2$
c_M = torque coefficient, $M = c_M \pi R^3 \rho(\omega R)^2$
c_P = power coefficient, $P = c_P \pi R^3 \rho(\omega R)^3$
a = slope of the curve of section lift coefficient against angle of attack
c = blade chord
b = number of blades
θ_t = pitch angle of the blade tip; θ at a radius r
ϕ_t = inflow angle of the blade tip; ϕ at a radius r
σ = solidity = $b\ c\ R/\pi R^2$
∂ = average blade profile - drag coefficient
$\tilde{c}_L$ = mean lift coefficient
x = r/R
α = turbine blade angle; blade angle of attack; flapping angle
c_d = section profile - drag coefficient
L = lift, N
D = drag, N
Δw = peripheral change of velocity, m/s
ξ = cross section coefficient of utilization.

SUBSCRIPTS

c = compressor; climb
1 = ambient condition; internal rotor ring
2 = compressor exit; external rotor ring
t = turbine; rotor blade tip
3, 4, 5, 6 = turbine stations as in figure 8
A = aircraft
R = rotor
W = weight
F = forward

REFERENCES

1) D. Dini: Prediction of Aeroelastic Instabilities in Rotorcraft Engine. Presented at the AGARD Conference Proceedings No. 248, Cleveland.

2) A. Gessow and G.C. Myers: Aerodynamics of the Helicopters. Frederick Ungar Publishing Co., New York, 1967.

3) P. Brotherhood: An Investigation in Flight of the Induced Velocity Distribution under a Helicopter Rotor when Hovering. Br. ARC RAE Rep. No. Aero. 2212, June 1947.

4) H. Glauert: Airplane Propellers, Vol. IV, Div. L of "Aerodynamic Theory". W.F. Durand, ed., Julius Springer, Berlin, 1935.

5) D.C. Gilmore and I.S. Gartshore: The Development of an Efficient Hovering Propeller/Rotor Performance Prediction Method. Presented at the AGARD Conference Proceedings No. 111, Marseilles, September 1972.

6) H.R. Young and D.R. Simon: The Advancing Blade Concept (ABC) Rotor Program. Presented at AGARD Conference Proceedings No. 233, NASA Ames Research Center, Moffett Field, California, May 1977.

7) D. Dini: Problems of Engine Response during Transient Maneuvers. Presented at the AGARD Conference Proceedings No. 302 on Helicopter Propulsion Systems, Toulouse, 11 - 14 May 1981.

8) D. Dini: Rotor - Fuselage Interference on Engine Internal Aerodynamics in Maneuvering High - Speed Rotorcraft. Presented at the AGARD FDP 50th Panel Meeting/Specialists' Meeting on Prediction of Aerodynamic Loads on Rotorcraft, London 17 - 21 May 1982.

ACKNOWLEDGEMENTS

The author wishes to grateful acknowledge the contribution made by Mrs. Gigliola Cei and Mr. Salvatore Fiorini in typewriting and drawing the present paper.